Optical-quality controllable wet-chemical doping of graphene through a uniform, transparent and low-roughness F4-TCNQ/MEK layer

Supplementary material

Misseeuw, Lara; Krajewska, Aleksandra; Pasternak, Iwona; Ciuk, Tymoteusz; Strupinski, Wlodek; REEKMANS, Gunter; ADRIAENSENS, Peter; GELDOF, Davy; Blockhuys, Frank; Van Vlierberghe, Sandra; Thienpont, Hugo; Dubruel, Peter & Vermeulen, Nathalie (2016) Optical-quality controllable wet-chemical doping of graphene through a uniform, transparent and low-roughness F4-TCNQ/MEK layer. In: RSC ADVANCES, 6(106), p. 104491-104501.

DOI: 10.1039/c6ra24057g
Handle: http://hdl.handle.net/1942/23043

SUPPLEMENTARY INFORMATION

Optical-quality Controllable Wet-Chemical Doping of Graphene through a Uniform, Transparent and Low-Roughness F4-TCNQ/MEK Layer

Lara Misseeuw[a*], *Aleksandra Krajewska*[b,c], *Iwona Pasternak*[c], Tymoteusz *Ciuk*[c], *Wlodek Strupinski*[c], *Gunter Reekmans*[d], *Peter Adriaensens*[d], *Davy Geldof*[e], *Frank Blockhuys*[e], *Sandra Van Vlierberghe*[a,e,f], *Hugo Thienpont*[a], *Peter Dubruel*[f], *Nathalie Vermeulen*[a]

a. Brussels Photonics Team (B-PHOT), Dept. of Applied Physics and Photonics (IR-TONA), Vrije Universiteit Brussel, Pleinlaan 2, B-1050 Brussels, Belgium
*lmisseeu@b-phot.org

b. Institute of Optoelectronics, Military University of Technology, Gen. S. Kaliskiego 2, 00-908 Warsaw, Poland

c. Institute of Electronic Materials Technology, Wolczynska 133, 01-919 Warsaw, Poland

d. Applied and Analytical Chemistry, Institute for Materials Research (IMO), Hasselt University, Agoralaan 1-Building D, BE-3590 Diepenbeek, Belgium

e. Department of Chemistry, University of Antwerp, Groenborgerlaan 171, B-2020 Antwerp, Belgium

f. Polymer Chemistry & Biomaterials Research Group, Ghent University, Krijgslaan 281 (S4 Bis), Ghent B-9000, Belgium

EXPERIMENTAL METHODS

Preparation of the dopant solutions

In order to examine the solubility of F4-TCNQ, F4-TCNQ (Sigma Aldrich, 97%) was added to different solvents: toluene, chloroform, DMSO, xylene, isopropyl alcohol, trichlorobenzene, acetonitrile, dichloromethane (DCM), dioxane, butan-2-one (methyl ethyl ketone or MEK), acetone, 3-methyl-butan-2-one, 4-methyl-pentan-2-one, pentan-3-one and cyclohexanone (all solvents are from Sigma Aldrich, except isopropyl alcohol which is from Chem-lab and cyclohexanone from Merck).

To analyze the concentration dependence of the doping effect of F4-TCNQ dissolved in MEK (≥ 99.7% HPLC grade), different quantities of F4-TCNQ ranging from 1 to 40 mg/ml were solubilized (volume: 2 ml). All solutions were stirred (100 rpm) and heated (at 50°C) for a certain time depending on the concentration (see section 3.1.1).

Characterization of the dopant solution

To elucidate the chemical interactions between F4-TCNQ and the solvent, Nuclear Magnetic Resonance (NMR) spectroscopy was applied, on the one hand to F4-TCNQ powder and on the other hand to solutions of F4-TCNQ. The ^{19}F solid-state NMR spectrum of F4-TCNQ was acquired on a 400 MHz Varian VNMRS DirectDrive spectrometer, equipped with a 3.2 mm T3HX probe under magic angles spinning (MAS) at 17 kHz. The chemical shift scale (δ) in ppm was calibrated relative to ammoniumtrifluoroacetate at -72.0 ppm. Acquisition parameters used were: a spectral width of 200 kHz, an acquisition time of 15 ms, a pulse length of 10 µs, a preparation delay time of 20 s and 200 accumulations. A line-broadening of 50 Hz was applied before Fourier transformation. Subsequently, ^{19}F liquid-state NMR spectra of the dopant solutions were acquired on a 400 MHz Varian Inova spectrometer with a 5 mm OneNMR probe. Hereto, 700 µl of a 20 mg/ml F4-TCNQ solution was mixed with 10% (v/v) $CDCl_3$. The ppm scale was calibrated relative to trifluorotoluene at -63.72 ppm. Free induction decays were collected with a 45° pulse of 4.0 µs, a spectral width of 78 kHz, an acquisition time of 0.5 s, a preparation delay of 4 s and 100-400 accumulations. A line-broadening of 5 Hz was applied before Fourier transformation. Additionally, a ^{19}F COSY 2D spectrum was obtained with 4 accumulations for each of the 256 increments in the t_1 time domain, resulting in a total acquisition time of 20

minutes. The spectral width in the F1 and F2 dimension was 7600 Hz and a sine bell function was applied in the two dimensions. Finally, the ^{13}C NMR spectra[1] were measured on the same spectrometer and with the same probe. Hereto, 40 mg F4-TCNQ was dissolved in 700 µl solvent supplemented with 10% (v/v) $CDCl_3$. The ppm scale was calibrated relative to $CDCl_3$ at 77.7 ppm. Free induction decays were collected with a 90° pulse of 8.0 µs, a spectral width of 25 kHz, an acquisition time of 1.0 s, a preparation delay of 300 s and 1000 accumulations. A line-broadening of 5 Hz was applied before Fourier transformation.

The dopant solutions were also characterized optically by measuring their absorbance through UV-VIS spectroscopy (Uvikon, BIO-TEK instruments, 1 ml solution).

Spincoating of the dopant solution

The spincoating technique was applied to deposit F4-TCNQ on different substrates. To investigate the deposition itself without considering the doping effect on graphene, the dopant solutions were initially spincoated on a) highly resistive Si samples (R > 1000 Ω cm, purchased from PI KEM) with a surface of 1 cm x 1 cm and a thickness of 500 µm and b) glass slides with a surface of 5 cm^2 and a thickness of 140 µm. The spin parameters were the following: 5000 rpm, 1500 rpm/s acceleration, 25 s spin time and 5 µl (for the Si samples) or 25 µl volume (for the glass slides). In a later stage, to test the actual doping effect on graphene, the same spincoating parameters were used to spincoat the dopant layer on top of graphene using a volume of 5 µl.

Analysis of the spincoated layer

The quality of the spincoated depositions was characterized with atomic force microscopy (AFM) to study the surface morphology (expressed in RMS roughness), using a multimode scanning probe microscope (Digital Instruments) equipped with a Nanoscope IIIa controller. The scanned surface was 25 μm^2 and recorded in tapping mode with a scan rate of 0.2 Hz with a silicon cantilever (OTESPA-Veeco). Nanoscope software version 4.43r8 was used for surface roughness analysis after the recorded images were modified with an X and Y Plane Fit Auto procedure. Furthermore, we performed X-ray Photo-electron Spectroscopy (XPS) measurements on four random

locations on a bare Si sample (reference) and on a Si sample spincoated with the dopant solution to verify the composition and homogenity of the layer (ESCA S-probe VG monochromatic spectrometer with an Al K_α X-ray source (1486 eV), recorded with a spot size of 250 μm by 1000 μm and analyzed using Casa XPS software package). In order to quantify the transparency of the layers, optical transmission measurements were carried out for the dopant layers spincoated on the glass slides (Jasco V-670 UV-VIS/NIR Spectrophotometer over the wavelength range from 550 to 1900 nm, including both the VIS (visible spectrum) and NIR (near infrared)). The layer thickness of spincoated F4-TCNQ/MEK layers for different concentrations at a spinspeed of 5000 rpm on Si substrates was determined with ellipsometry (J.A. Woollam Co., M-2000).

Quantum chemical calculations

To obtain insight in the nature of the interaction between F4-TCNQ and MEK, quantum chemical calculations were performed using the Gaussian 09 suite of programs[2] applying the B3LYP and ωB97XD functional and the 6-311++G** basis set, as they are implemented in the program. After each geometry optimization, a force-field calculation was carried out to verify that the obtained structure corresponded to a minimum on the Potential Energy Surface (PES). Atomic charges (and the resulting charge transfer between the fragments) were calculated using the Fractional Occupation Hirshfeld Iterative (FOHI) formalism.[3] The Basis Set Superposition Error (BSSE) was estimated using the counterpoise method implemented in Gaussian 09. The Integral Equation Formalism Polarized Continuum Model (IEFPCM) was used as it is implemented in Gaussian 09 to simulate solutions rather than gas phase components. Note that Gaussian 09 does not allow the calculation of the BSSE when PCM is used.

Graphene growth

The doping method was investigated on two types of graphene. The first one was p-type hydrogen-intercalated quasi-free-standing monolayer graphene, grown in an epitaxial chemical vapor deposition (CVD) process on the Si-face of 6H-SiC(0001) substrates[4], with a surface of 1 cm x 1 cm. The second type was monolayer graphene, provided by CVD growth of carbon on copper[5] and transferred on Si samples (highly

resistive R > 1000 Ω cm, purchased from PI KEM) with a surface of 1 cm x 1 cm by electrochemical delamination.[6,7]

Graphene doping quantification

To quantify the doping effect, the electrical parameters of graphene (i.e. charge carrier concentration (n in cm^{-2}), mobility (μ in $cm^2 V^{-1} s^{-1}$) and sheet resistance (R in Ω/sq)) were measured before and after doping (i.e. after spincoating a F4-TCNQ/MEK layer on top of graphene) with a Hall effect measurement system in van der Pauw geometry (0.55T Ecopia HMS-3000 Hall setup). Indium contacts were placed in the corners of the graphene-covered samples to perform a four-point probe measurement, so that after depositing the electrically insulating dopant layer, it was still possible to measure the electrical current through the graphene layer.

In addition, Raman spectroscopy measurements (LabRAM HR Evolution (HORIBA Scientific), HeNe laser light source at 633 nm and with a laser power of 5 mW) were performed on graphene, that is CVD grown on copper and transferred on Si samples, before and after doping with an F4-TCNQ/MEK layer.

^{13}C-NMR SPECTRA OF F4-TCNQ DOPANT SOLUTIONS

Figures S1a and b show the ^{13}C-NMR spectrum of F4-TCNQ dissolved in MEK and acetonitrile, respectively. A first difference can be found in the chemical shift of the fluorinated carbons, which is around 145 ppm for ketone solvents like MEK and 142 ppm for acetonitrile. This points to different interactions between F4-TCNQ and the solvents. We remark that the splitting of the fluorinated carbons is due to carbon-fluorine J-couplings (mainly the large $^1J_{C-F}$ and smaller $^2J_{C-F}$). Furthermore, the asymmetric unit cell of F4-TCNQ is not reflected in the carbon spectra.

A second difference can be observed for the other carbon signals: whereas the peaks are sharp in the spectrum of F4-TCNQ in MEK, no sharp peaks are observed for F4-TCNQ in acetonitrile due to severe broadening (i.e. increasing $\nu_{1/2}$) as a result of increasing (paramagnetic) T_2 relaxation caused by the unpaired electron of the negatively ionized F4-TCNQ (see section 3.1.3). Since the rate of T_2 relaxation is strongly dependent on the distance r to the unpaired electron (~ $1/r^6$), and since almost only the fluorinated carbon signals are observed in the spectrum, the unpaired

electron must be situated on the nitrogen of the nitrile groups. Remark further that the spectrum for F4-TCNQ in MEK shows more signals than one would expect for the three types of non-fluorinated carbons (represented as carbon atoms b, c and d in figure S1), indicating that the symmetry of F4-TCNQ is disturbed by interactions with the MEK solvent.

A third and major difference can be found for the solvent peaks in the ^{13}C-NMR spectra. For acetonitrile, only the expected solvent peak for pure acetonitrile is observed. However, zooming in on the carbonyl region of MEK (Figure S2) clearly shows that, compared to the main signal of pure MEK around 207.2 ppm, two additional upfield MEK signals appear in the spectrum upon dissolving F4-TCNQ. These additional carbonyl signals result from MEK molecules involved in specific interactions with F4-TCNQ.

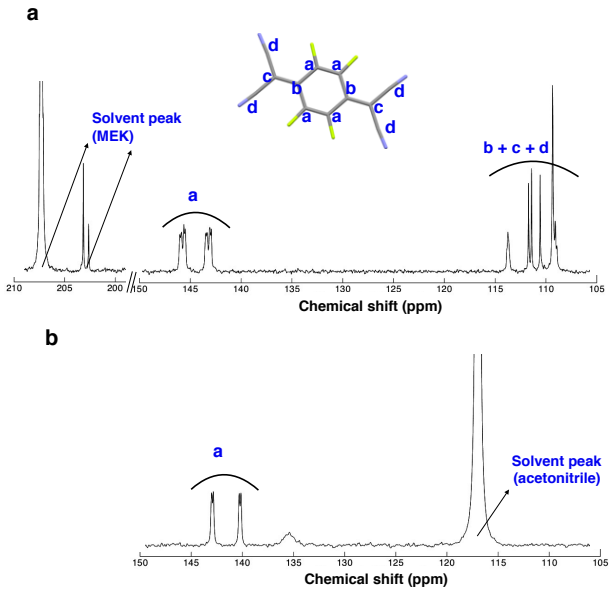

Figure S1. ^{13}C-NMR spectra of F4-TCNQ dissolved in (a) MEK and (b) acetonitrile . The inset represents a F4-TCNQ molecule with nitrogen atoms indicated in blue and fluorine atoms indicated in green colors.

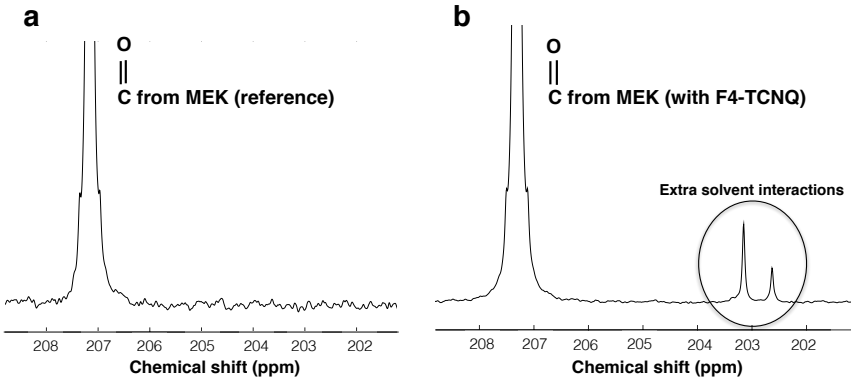

Figure S2. Zoom in on the carbonyl signal of (a) free MEK as a reference and (b) MEK upon dissolving F4-TCNQ.

LAYER THICKNESS OF SPINCOATED F4-TCNQ/MEK LAYERS

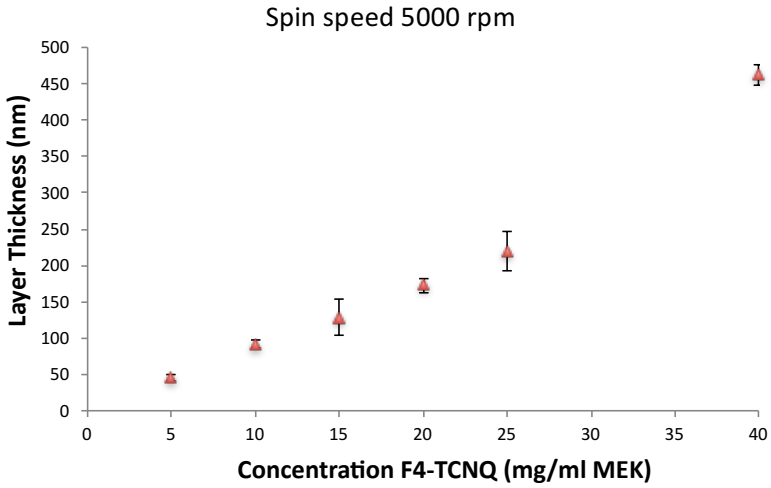

Figure S3. Layer thickness of F4-TCNQ/MEK layers for different concentrations F4-TCNQ spincoated (at a spin speed of 5000 rpm) on Si substrates.

The coverage of the F4-TCNQ molecules dissolved in MEK on the graphene surface is estimated in the following way: since it is known that F4-TCNQ is able to take up 0.4 electrons per molecule[8] and the size of the molecule[9] equals 0.975 nm^2, a doping level of Δn = 1E13 cm^{-2} corresponds to 2.5E13 F4-TCNQ molecules per cm^2 and as such a coverage level of 24%.

TABLES WITH ELECTRICAL PARAMETERS OF GRAPHENE SAMPLES BEFORE AND AFTER DOPING CHARACTERIZED THROUGH HALL EFFECT MEASUREMENTS

Table S1. The electrical parameters n, μ and R for six different samples of epitaxial graphene (quasi-free-standing on SiC substrates (6H)) before and after doping with an F4-TCNQ/MEK layer when varying the concentration of F4-TCNQ from 2.5 to 40 mg/ml MEK.

	Concentration Charge Carriers			Mobility			Sheet Resistance		
Concentration (mg F4-TCNQ/ ml MEK)	n_{before} (cm^{-2})	n_{after} (cm^{-2})	Δn (cm^{-2})	μ_{before} ($cm^2V^{-1}s^{-1}$)	μ_{after} ($cm^2V^{-1}s^{-1}$)	$\Delta\mu$ ($cm^2V^{-1}s^{-1}$)	R_{before} (Ω/sq)	R_{after} (Ω/sq)	ΔR (Ω/sq)
2.5	9,24E+12	1,83E+13	9,10E+12	1991	1126	-865	339	302	-37
5	9,09E+12	2,00E+13	1,09E+13	3847	1708	-2139	179	183	4
7.5	9,91E+12	2,16E+13	1,17E+13	2054	1575	-479	307	184	-123
10	1,07E+13	2,08E+13	1,01E+13	2874	1532	-1342	203	196	-7
20	1,06E+13	1,95E+13	8,93E+12	1757	1524	-233	335	210	-125
40	1,11E+13	1,72E+13	6,07E+12	1959	1651	-308	286	221	-65

Table S2. The electrical parameters n, μ and R for eight different samples of graphene (CVD grown on copper and transferred to Si substrates) before and after doping with an F4-TCNQ/MEK layer when varying the concentration of F4-TCNQ from 1 to 40 mg/ml MEK.

	Concentration Charge Carriers			Mobility			Sheet Resistance		
Concentration (mg F4-TCNQ/ ml MEK)	n_{before} (cm^{-2})	n_{after} (cm^{-2})	Δn (cm^{-2})	μ_{before} (cm^2V^{-1} s^{-1})	μ_{after} (cm^2V^{-1} s^{-1})	Δμ (cm^2V^{-1} s^{-1})	R_{before} (Ω/sq)	R_{after} (Ω/sq)	ΔR (Ω/sq)
1	4.79E12	9.68E12	4.89E12	1612	1257	-355	808	513	-295
2.5	3.15E12	1.28E13	9.68E12	2141	1123	-1018	927	433	-494
5	4.13E12	1.43E13	1.02E13	1698	995	-703	891	438	-453
7.5	5.40E12	1,69E+13	1.15E13	1395	767	-628	829	483	-346
10	4.60E12	1.42E13	9.62E13	1129	722	-407	1197	608	-589
20	4.30E12	1.30E13	8.69E12	1554	849	-705	934	506	-428
30	4.96E12	1.11E13	6.12E12	755	692	-63	1666	815	-851
40	4.77E12	1.04E13	5.66E12	1385	1136	-249	945	527	-418

CHANGE IN SHEET CONDUCTANCE OF GRAPHENE (CVD GROWN ON COPPER AND TRANSFERRED TO SI SUBSTRATES) AFTER DOPING WITH AN F4-TCNQ/MEK LAYER

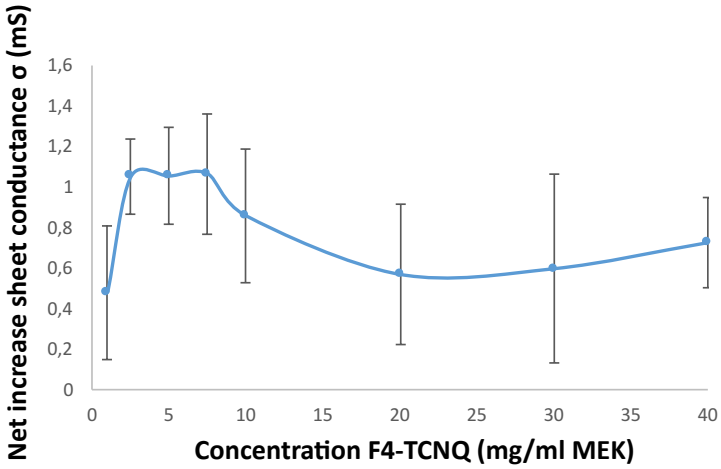

Figure S4. Change in sheet conductance of graphene (CVD grown on copper and transferred to Si substrates) after doping with an F4-TCNQ/MEK layer when varying the concentration of F4-TCNQ from 1 – 40 mg/ml MEK

The sheet conductance for graphene on silicon samples is increasing after doping as a result of an increasing concentration charge carriers and decreasing sheet resistance. The same trend as for change in concentration charge carrier is observed, i.e. a maximum change at a concentration of 7.5 mg F4-TCNQ/ml MEK and decreasing doping effect for higher concentrations.

RAMAN SPECTROSCOPY MEASUREMENTS OF GRAPHENE (CVD GROWN ON COPPER AND TRANSFERRED TO SI SUBSTRATES) AFTER DOPING WITH AN F4-TCNQ/MEK LAYER

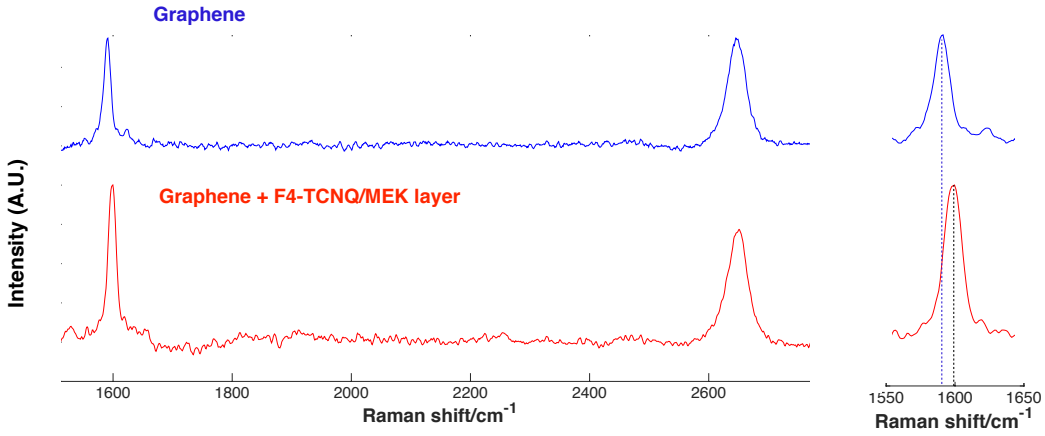

Figure S5. Raman spectroscopy measurements of graphene (CVD grown on copper and transferred to Si substrates) before and after doping with an F4-TCNQ/MEK layer with a concentration of 10 mg/ml (left) and zoom in of the G band (right).

Raman spectroscopy measurements of graphene before and after doping clearly show the p-doping effect of the F4-TCNQ/MEK layer by the frequency-upshifting of the G-band from 1592 cm^{-1} to 1600 cm^{-1} and of the 2D-band from 2647 cm^{-1} to 2650 cm^{-1}. As pointed out in reference 10 such an upshift in both the G-band and 2D-band is expected when applying p-doping to graphene.

REFERENCES

1 R. Rego, P. J. Adriaensens, R. A. Carleer and J. A. Gelan, *Polymer (Guildf).*, 2004, **45**, 33–38.

2 M. Frisch, G. W. Trucks, H. B. Schlegel, G. E. Scuseria, M. A. Robb, J. R. Cheeseman, G. Scalmani, V. Barone, B. Mennucci, G. A. Petersson and Others, *Inc., Wallingford, CT*, 2013.

3 D. Geldof, A. Krishtal, F. Blockhuys and C. Van Alsenoy, *J. Chem. Theory Comput.*, 2011, **7**, 1328–1335.

4 T. Ciuk and W. Strupinski, *Carbon*, 2015, **93**, 1042–1049.

5 K. S. Kim, Y. Zhao, H. Jang, S. Y. Lee, J. M. Kim, K. S. Kim, J.-H. Ahn, P. Kim, J.-Y. Choi and B. H. Hong, *Nature*, 2009, **457**, 706–10.

6 Y. Wang, Y. Zheng, X. Xu, E. Dubuisson, Q. Bao, J. Lu, K. P. Loh and W. E. T. Al, *ACS Nano*, 2011, **5**, 9927–9933.

7 T. Ciuk, I. Pasternak, A. Krajewska, J. Sobieski, P. Caban, J. Szmidt and W. Strupinski, *J. Phys. Chem. C*, 2013, **117**, 20833–20837.

8 S. Barja, M. Garnica, J. J. Hinarejos, A. L. Vázquez de Parga, N. Martín and R. Miranda, *Chem. Commun.*, 2010, **46**, 8198.

9 H.-Z. Tsai, A. A. Omrani, S. Coh, H. Oh, S. Wickenburg, Y. Son, D. Wong, A. Riss, H. S. Jung, G. D. Nguyen, G. F. Rodgers, A. S. Aikawa, T. Taniguchi, K. Watanabe, A. Zettl, S. G. Louie, J. Lu, M. L. Cohen and M. F. Crommie, *ACS Nano*, 2015, **9**, 12168-12173.

10 A Tiberj, M. Paillet, P. Landois, M. Mikolasek, S. Contreras, E. Dujardin, L. Charles, M. Rubio-Roy, J.-R. Huntzinger, J.-L. Sauvajol and A-A Zahab, *Sci. Rep.*, 2013, **3**, 1–6.